PHYSICAL REVIEW E, VOLUME 65, 025201(R)

Birhythmicity induced by perturbing an oscillating electrochemical system

M. Rivera and P. Parmananda
Facultad de Ciencias, UAEM, Avenida Universidad 1001, Col. Chamilpa, Cuernavaca, Morelos, Mexico

M. Eiswirth
Fritz-Haber-Institut der Max-Planck-Gesellschaft, Faradayweg 4-6, D-14195 Berlin, Germany
(Received 20 September 2001; published 17 January 2002)

We describe the generation of new limit cycles in electrochemical systems under the influence of external periodic perturbations. For certain specific parameters of a nonharmonic forcing function, two coexisting periodic orbits can be generated from a single limit cycle observed in the unperturbed dynamics. This inception of birhythmicity (bistability) is observed in both simulations and actual experiments involving potentiostatic electrodissolution of copper in an acetate buffer.

DOI: 10.1103/PhysRevE.65.025201 PACS number(s): 82.40.Bj, 82.45.Fk, 82.45.Qr

I. INTRODUCTION

Periodic forcing of oscillatory systems has been studied extensively in electrical [1,2], hydrodynamical [3], chemical [4–8], and biological [9,10] systems. It has been realized that for appropriate parameters of the superimposed perturbations, a plethora of dynamical behavior ranging over harmonic, quasiperiodic, and chaotic responses can be observed. However, there exists another aspect of interaction between autonomous oscillatory dynamics and applied periodic perturbations that has received much less attention. This involves the generation of multiple coexisting attractors in oscillating systems by superimposed periodic perturbations of a predetermined form [11,12]. The theoretical framework for this nonharmonic forcing-induced multistability was first provided by Loud [11]. Detailed deterministic analysis including numerical simulations was subsequently carried out by Rehmus *et al.* [12].

In this Rapid Communication, we revisit this phenomenon and test its validity in simulations and experiments involving electrochemical corrosion. Based on the prior work of Rehmus *et al.* [12], we devise appropriate forcing functions that result in the emergence of bistability, in both the model and the experiments. This paper is organized as follows. In Sec. II, we briefly summarize the theoretical framework presented by Loud and thereafter explicitly formulated by Rehmus *et al.* Section III includes numerical results indicating the emergence of bistability under appropriate periodic forcing. In Sec. IV, we present experimental results that illustrate the inception of bistability as a result of the interaction between autonomous system dynamics (limit cycle behavior) and superimposed periodic perturbations. The paper concludes with a short summary in Sec. V.

II. THEORETICAL BACKGROUND

Loud [11] proved analytically that limit cycle behavior subjected to external periodic perturbations may have multiple solutions. Building on the work of Loud, Rehmus *et al.* [12] provided a recipe for constructing appropriate forms of forcing functions that would result in the inception of multistability in system dynamics. Paraphrasing from their work, we define an autonomous system as

$$\dot{\mathbf{X}} = \mathbf{f}(\mathbf{X}, \mathbf{P}), \tag{1}$$

which, at appropriate values of the parameter vector ($\mathbf{P}$), exhibits limit cycle behavior. Denoting the stable periodic solution of the autonomous system as $\mathbf{X}_0(\omega_0 t)$, there exists a nontrivial matrix solution Ω of the linear variational problem evaluated at $\mathbf{X}_0(\omega_0 t)$. Under periodic forcing, the nonautonomous system is given by

$$\dot{\mathbf{X}} = \mathbf{f}(\mathbf{X}, \mathbf{P}) + b(\omega_p t, \mathbf{X}), \tag{2}$$

where b is the nonharmonic forcing function with the perturbation frequency ω_p chosen such that ω_0/ω_p is close to a rational ratio n/m. The solution to Eq. (2) is an indefinite integral [12] whose index i determines the number of new limit cycles generated. Rehmus *et al.* subsequently tested this concept in a numerical model simulating, continuously stirred tank reactor (CSTR) experiments. For observation of

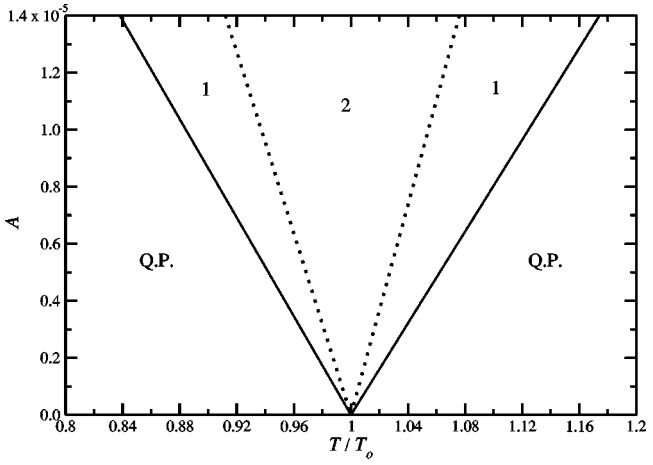

FIG. 1. Numerically constructed phase diagram showing the type of response as a function of amplitude and period of the superimposed perturbations. The numbers 1 and 2 within the entrainment band correspond to the regions of monostability and bistability, respectively.

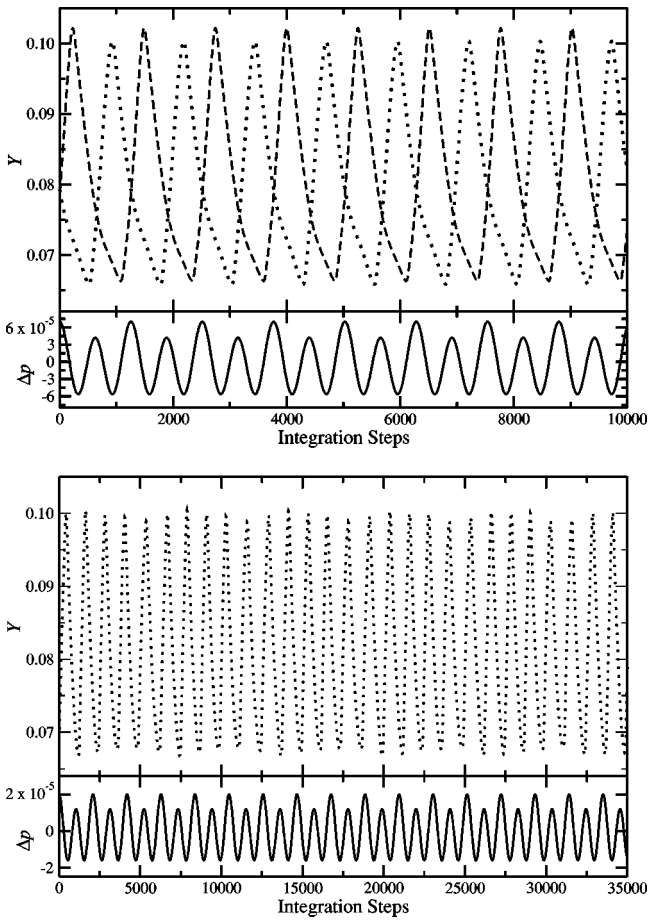

FIG. 2. (a) Time series of the coexisting periodic orbits generated under the influence of the external periodic perturbations. The perturbations that lead to their inception are also superimposed. The model parameters are $\{p,q,\beta\}$ $\{2.0\times10^{-4},1.0\times10^{-3},5.0\}$, respectively, and the forcing parameters are $A=1.4\times10^{-5}$, and $\omega=0.005$ rad/s. (b) Quasiperiodic time series and the forcing function responsible for their generation outside the entrainment band. The system parameters are the same as in (a) and the forcing parameters are $A=0.4\times10^{-5}$ and $\omega=0.003$ rad/s.

bistability, the appropriate waveform of the external periodic perturbations was calculated to be [12]

$$b(\omega(t))=A_1\cos(\omega_p t)+A_2\cos(2\omega_p t). \tag{3}$$

Furthermore, to induce tristability they used the following forcing function:

$$b(\omega(t))=A_1\cos(\omega_p t)+A_2\cos(3\omega_p t). \tag{4}$$

Their numerical results confirmed that forcing functions of Eqs. (3) and (4) could indeed introduce bistability and tristability (respectively) in the perturbed system [12].

Due to the anticipated problems with intrinsic noise (also addressed by Rehmus *et al.* [12]) in our experiments, we restricted our endeavors to a search for forcing-induced bistability.

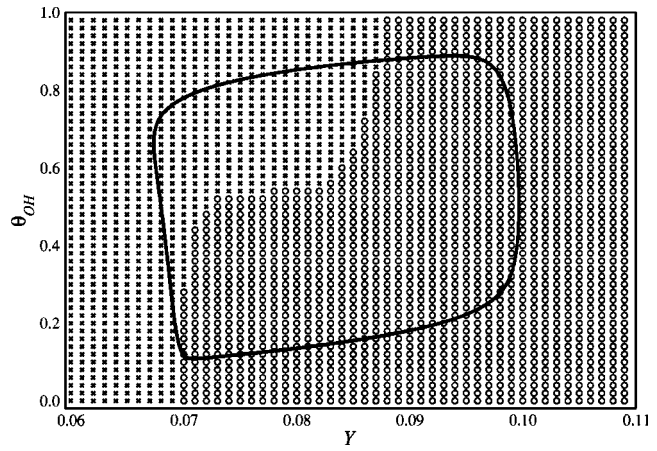

FIG. 3. State space portrait showing the basin of attraction for coexisting periodic attractors in the bistable region of the entrainment band. The parameters for the forcing function are $A=2\times10^{-5}$ and $\omega=0.005$ rad/s. Also superimposed is the autonomous limit cycle for the system parameters of Fig. 2(a).

A. Numerical results

As a precursor to examining birhythmicity induced by external periodic forcing in an actual electrochemical cell, we study it in a numerical model [13]. The model system, simulating aqueous electrochemical corrosion [13,14], is described by two dimensionless differential equations:

$$\dot{Y}=p(1-\theta_{\mathrm{OH}})-qY, \tag{5}$$

$$\dot{\theta}_{\mathrm{OH}}=Y(1-\theta_{\mathrm{OH}})-[\exp(-\beta\theta_{\mathrm{OH}})]\theta_{\mathrm{OH}}. \tag{6}$$

The variable θ_{OH} represents the fraction of the electrode surface covered by a metal hydroxide film, while Y represents the concentration of metal ions in the electrolytic solution. The parameters p,q, and β are determined by chemical reaction rates in the model. Previous numerical studies [14] have shown that this model exhibits limit cycle behavior for parameter set $\{p,q,\beta\}$ in the neighborhood of $\{2.0\times10^{-4},1.0\times10^{-3},5.0\}$ by virtue of an underlying supercritical Hopf bifurcation. We numerically integrated these equations using a fourth order Runge-Kutta algorithm with a constant step size of $h=1$. To induce bistability, the system parameter p was modulated continuously as follows:

$$p=p_0+\Delta p, \tag{7}$$

where,

$$\Delta p=A[\cos(\omega_p t)+4\cos(2\omega_p t)], \tag{8}$$

where $p_0=2.0\times10^{-4}$, so the autonomous system exhibits limit cycle behavior. The external perturbations were superimposed on p because it is related to the anodic potential V, an experimentally accessible control parameter. The general behavior of the model system under the influence of the periodic modulations with amplitude (A) and time period T (scaled relative to the natural time period T_0 of the period-1 oscillation) is schematically represented by the phase diagram in Fig. 1. The response of the periodically perturbed

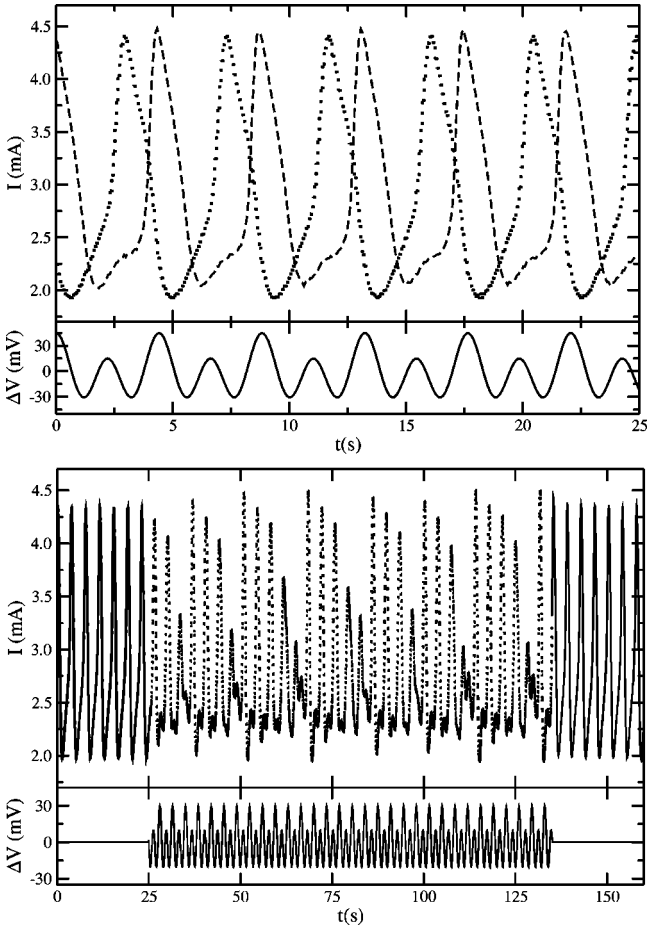

FIG. 4. (a) Time series of anodic current I for the coexisting periodic orbits generated via periodic perturbation of the anodic voltage V. The system parameters for the experiments are $V_0 = 660$ mV and 1300 rpm, and the forcing parameters are $A = 15$ mV and $\omega = 1.43$ rad/s. (b) Quasiperiodic behavior of anodic current I and the forcing function responsible for its generation. The experimental parameters are the same as in (a) and the forcing parameters are $A = 10$ mV and $\omega = 1.8$ rad/s.

system exhibits monostability, bistability, and quasiperiodicity as indicated by the demarcated regions in the phase diagram. Figure 2(a) shows the time series for the two periodic attractors generated in the perturbed system along with the wave form of the periodic forcing. Depending on the location within the entrainment band, these generated attractors can coexist or exist independently. A typical time series for the quasiperiodic behavior observed outside the entrainment band is shown in Fig. 2(b). This quasiperiodic nature of the system dynamics was also verified (results not shown) using return map reconstruction and Fourier analysis. Figure 3 shows a state space portrait for the perturbed system corresponding to the bistable region in the entrainment band. It depicts the basins of attraction for the two coexisting periodic attractors along with the limit cycle of the unperturbed system.

III. EXPERIMENTAL RESULTS

The experimental system was a PAR Model K60066 (Princeton Applied Research) three-electrode electrochemical cell set up to study the potentiostatic electrodissolution of copper in an acetate buffer. Under appropriate parameter conditions, this electrochemical system exhibits both periodic and chaotic current oscillations [15,16]. The anode is a rotating copper disk (5 mm diam) shrouded by Teflon. The electrolyte solution was an acetate buffer, a mixture consisting of 70 parts glacial acetic acid and 30 parts 2M sodium acetate. A volume of about 100 ml was maintained in the cell. The anodic potential (V) measured relative to a saturated calomel reference electrode (SCE) was used as the perturbation parameter on which the external periodic forcing was superimposed. The cathode was 2.5 cm^2 platinum foil. Oscillations in anodic current (the current between the anode and the cathode) were recorded using a 12-bit data acquisition card. Typical periods for the current oscillations ranged between 4 and 7 sec depending on experimental conditions and system parameters. To induce birhythmicity, the anodic voltage V was perturbed as follows:

$$V = V_0 + \Delta V, \tag{9}$$

where

$$\Delta V = A[\cos(\omega_p t) + 2\cos(2\omega_p t)], \tag{10}$$

where V_0 is chosen such that the autonomous system exhibits oscillations in the anodic current I (period-1) with a characteristic frequency ω_0. Figure 4(a) shows the time series of the coexisting period-1 current oscillations. They were obtained by initiating forcing of the anodic voltage at different phases of the autonomous period-1 current oscillation. Similarly to Fig. 1, variation of ω_p at a constant amplitude (A) divulges parameter domains of monostability, bistability, and quasiperiodicity. Figure 4(b) shows the quasiperiodic time series generated by an appropriate forcing function. The experimental return map constructed for the quasiperiodic dynamics is shown in Fig. 5. It reveals the quasiperiodic nature of the observed dynamics since the experimental Poincaré

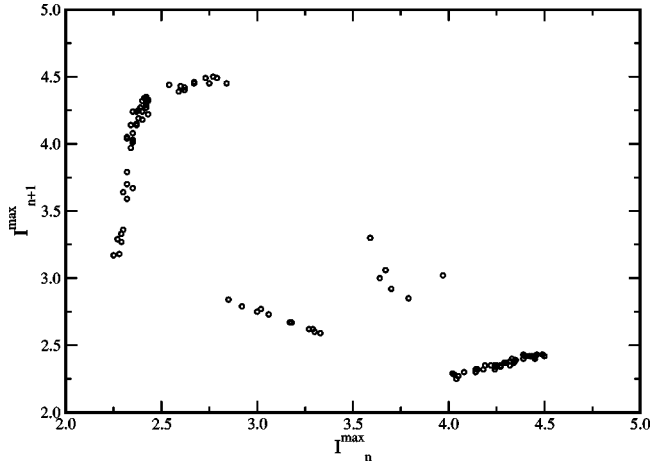

FIG. 5. Return map constructed using successive maxima for the time series of Fig. 4(b), as is characteristic of quasiperiodic dynamics.

section (return map) is a closed curve. The Fourier spectrum (not shown) was also characteristic of quasiperiodic dynamics.

IV. SUMMARY

This work describes experimental results verifying the induction of birhythmicity/bistability under the influence of periodic perturbations in agreement with a numerical model simulating electrochemical corrosion. Using the prescription provided by Rehmus *et al.* [12], we were able to identify regions of the phase diagram where the response of the perturbed system was entrained (phase locked) or quasiperiodic. Furthermore, within the entrainment band, regions of monostability and bistability are clearly demarcated.

ACKNOWLEDGMENTS

Two of us (M.R and P.P) acknowledge continuing support from CONACyT (Mexico).

[1] W.J. Yeh, D.R. He, and Y.H. Kao, Phys. Rev. Lett. **52**, 480 (1984).
[2] S. Martin and W. Martienssen, Phys. Rev. Lett. **56**, 1522 (1986).
[3] J. Maurer and A. Libchaber, J. Phys. (France) Lett. **40**, 419 (1979).
[4] F. Buchholtz and F.W. Schneider, J. Am. Chem. Soc. **105**, 7540 (1983)
[5] J.L. Hudson, P. Lamba, and J.C. Mankin, J. Phys. Chem. **90**, 3430 (1986).
[6] P. Lamba and J.L. Hudson, Chem. Eng. Sci. **42**, 1 (1987).
[7] M.M. Dolnik, E. Padusakaýa, and M. Marek, J. Phys. Chem. **91**, 4407 (1987).
[8] M. Eiswirth and G. Ertl, Phys. Rev. Lett. **60**, 1526 (1988).
[9] K. Aihara, G. Matsumoto, and Y. Ikegaya, J. Theor. Biol. **109**, 249 (1984).
[10] L. Glass, M.R. Guevara, J. Belair, and A. Shrier, Phys. Rev. A **29**, 1348 (1984).
[11] W.S. Loud, Ann. Math. **70**, 490 (1959).
[12] P. Rehmus, W. Vance, and J. Ross, J. Chem. Phys. **80**, 3373 (1984).
[13] J.B. Talbot and R.A. Oriani, Electrochim. Acta **30**, 1277 (1985).
[14] A.J. Markworth, J.K. McCoy, R.W. Rollins, and P. Parmananda, in *Applied Chaos*, edited by J.H. Kim and J. Stringer (John Wiley & Sons, Inc., New York, 1992).
[15] H.D. Dewald, P. Parmananda, and R.W. Rollins, J. Electroanal. Chem. Interfacial Electrochem. **306**, 297 (1991).
[16] H.D. Dewald, P. Parmananda, and R.W. Rollins, J. Electrochem. Soc. **140**, 1969 (1993).